



# PHB Biosynthesis Counteracts Redox Stress in *Herbaspirillum seropedicae*

Marcelo B. Batista<sup>1,2†</sup>, Cícero S. Teixeira<sup>1†</sup>, Michelle Z. T. Sfeir<sup>1</sup>, Luis P. S. Alves<sup>1</sup>, Glaucio Valdameri<sup>3</sup>, Fabio de Oliveira Pedrosa<sup>1</sup>, Guilherme L. Sasaki<sup>1</sup>, Maria B. R. Steffens<sup>1</sup>, Emanuel M. de Souza<sup>1</sup>, Ray Dixon<sup>2</sup> and Marcelo Müller-Santos<sup>1\*</sup>

<sup>1</sup> Department of Biochemistry and Molecular Biology, Universidade Federal do Paraná, Curitiba, Brazil, <sup>2</sup> Department of Molecular Microbiology, John Innes Centre, Norwich, United Kingdom, <sup>3</sup> Department of Clinical Analysis, Universidade Federal do Paraná, Curitiba, Brazil

## OPEN ACCESS

### Edited by:

Martin Koenneke,  
Universität Bremen, Germany

### Reviewed by:

Daniel Segura,  
Universidad Nacional Autónoma  
de México, Mexico  
Erhard Bremer,  
University of Marburg, Germany

### \*Correspondence:

Marcelo Müller-Santos  
marcelomuller@ufpr.br

† These authors have contributed  
equally to this work.

### Specialty section:

This article was submitted to  
Microbial Physiology and Metabolism,  
a section of the journal  
Frontiers in Microbiology

Received: 29 December 2017

Accepted: 28 February 2018

Published: 15 March 2018

### Citation:

Batista MB, Teixeira CS, Sfeir MZT,  
Alves LPS, Valdameri G,  
Pedrosa FO, Sasaki GL,  
Steffens MBR, de Souza EM,  
Dixon R and Müller-Santos M (2018)  
PHB Biosynthesis Counteracts Redox  
Stress in *Herbaspirillum seropedicae*.  
Front. Microbiol. 9:472.  
doi: 10.3389/fmicb.2018.00472

The ability of bacteria to produce polyhydroxyalkanoates such as poly(3-hydroxybutyrate) (PHB) enables provision of a carbon storage molecule that can be mobilized under demanding physiological conditions. However, the precise function of PHB in cellular metabolism has not been clearly defined. In order to determine the impact of PHB production on global physiology, we have characterized the properties of a  $\Delta phaC1$  mutant strain of the diazotrophic bacterium *Herbaspirillum seropedicae*. The absence of PHB in the mutant strain not only perturbs redox balance and increases oxidative stress, but also influences the activity of the redox-sensing Fnr transcription regulators, resulting in significant changes in expression of the cytochrome c-branch of the electron transport chain. The synthesis of PHB is itself dependent on the Fnr1 and Fnr3 proteins resulting in a cyclic dependency that couples synthesis of PHB with redox regulation. Transcriptional profiling of the  $\Delta phaC1$  mutant reveals that the loss of PHB synthesis affects the expression of many genes, including approximately 30% of the Fnr regulon.

**Keywords:** polyhydroxyalkanoates, Fnr, redox regulation, bacterial signal transduction, transcriptomics

## INTRODUCTION

*Herbaspirillum seropedicae* SmR1 is a nitrogen-fixing bacterium able to interact with important crops (Chubatsu et al., 2011; Pedrosa et al., 2011). The genome of this diazotroph harbors genes encoding homologs of PHA (polyhydroxyalkanoate) synthases in addition to other essential genes for PHA metabolism (Pedrosa et al., 2011; Tirapelle et al., 2013; Batista et al., 2016). The PHA synthase encoded by *phaC1* (Locus Tag: Hsero\_2999; Ref seq: YP\_003776395.1) is essential for poly(3-hydroxybutyrate) (PHB) synthesis in *H. seropedicae* SmR1 (Tirapelle et al., 2013; Alves et al., 2016). Other putative PHA synthase homologs present in the genome are *phaC2* (Locus Tag: Hsero\_2405; Ref Seq: YP\_003775812.1) and *phaC3* (Locus Tag: Hsero\_0265; Ref Seq: YP\_003773699.1). Phylogenetic analysis of *H. seropedicae* PhaC-like proteins (Batista et al., 2016) revealed that PhaC2 and PhaC3 group in the same clades as PhaC2 and PhaC5 from *Bradyrhizobium japonicum* USD110, respectively, both of which have no apparent role in PHB synthesis (Quelas et al., 2013). Thus *H. seropedicae* PhaC2 and PhaC3 may not be physiologically

important for PHB production (Batista et al., 2016). The most common PHA produced by bacteria, in general, is PHB (Lopez et al., 2015), which is accumulated as granules in the cytoplasm under conditions of carbon excess and limitation of other elements, such as oxygen or nitrogen (Madison and Huisman, 1999). The biosynthesis of PHB relies on the central carbon metabolite acetyl-CoA. In the first step of the synthesis, two molecules of acetyl-CoA are condensed by a  $\beta$ -ketothiolase (PhaA), to form acetoacetyl-CoA, which is then reduced to (R)-3-hydroxybutyryl-CoA by an acetoacetyl-CoA reductase (PhaB). Finally, the (R)-3-hydroxybutyryl-CoA is polymerized by the PHA synthase (PhaC) (Rehm, 2003). Recent studies have revealed that the metabolic role of PHAs is more complex than just providing an intracellular carbon store that can be mobilized to give enhanced competitiveness to PHA-producing bacteria. To date, PHA synthesis has been correlated with protective mechanisms against a diverse range of stress conditions, such as growth in the presence of oxidants, osmotic shock, resistance to desiccation, heat, and UV irradiation (Kadouri et al., 2003; Lopez et al., 2015; Koskimäki et al., 2016; Sacomboio et al., 2017). Additionally, PHA has been suggested to be important for maintaining the redox balance of the cell (Stockdale et al., 1968; Senior et al., 1972). In this study, we have investigated the physiological consequences of PHB synthesis in *H. seropedicae* by characterizing a mutant strain lacking *phaC1*, which is unable to produce PHB (Tirapelle et al., 2013). Under conditions of oxygen limitation, we observe that this mutation influences NAD(P)H/NAD(P)<sup>+</sup> ratios and increases susceptibility to oxidative stress, particularly to the superoxide propagator methyl viologen. This, in turn, impairs the activity of the redox-responsive transcriptional regulators Fnr1 and Fnr3, which are required for expression of the cytochrome c branch of the electron transport chain (ETC; Batista et al., 2013). As a consequence, the bacterium is unable to trigger effective adaptation to the shortage of oxygen and accommodate the change in redox balance. We also demonstrate that the Fnr proteins regulate the production of PHB. Thus, we have uncovered a cyclic dependency between PHB synthesis and Fnr activity that ensures reciprocal control of the redox balance under oxygen-limiting conditions.

## MATERIALS AND METHODS

### Strains and Plasmids

The bacterial strains and plasmids used in this study are listed in Supplementary Table 1.

### Culture Media, Growth Conditions, and Growth Rate Determinations

The *H. seropedicae* strains were grown under 30°C in NFbHPN-Malate medium supplemented with 20 mM NH<sub>4</sub>Cl (Klassen et al., 1997) in two different agitation rates to ensure low aeration (120 rpm) or high aeration (350 rpm). The sensitivity of *H. seropedicae* strains to methyl viologen (a superoxide propagator) was tested using cells grown to an OD<sub>600nm</sub> of 0.5, when different concentrations of

methyl viologen were added to the culture. Samples were taken at regular intervals to evaluate cell growth. Control cultures without addition of a reactive oxygen species (ROS) source were run in parallel. Antibiotic concentrations used for *H. seropedicae* were 80  $\mu$ g/mL for streptomycin, 500  $\mu$ g/mL for kanamycin and 10  $\mu$ g/mL for tetracycline. The growth rate ( $\mu$ ) for each condition was calculated as  $\mu = [\ln(\text{OD}_{600\text{nm}} \text{ at } t_1) - \ln(\text{OD}_{600\text{nm}} \text{ at } t_0)] / (t_1 - t_0)$  using the values of turbidity measurements during the exponential phase (Chavarria et al., 2013).

### Determination of Intracellular NAD(P)H and NAD(P)<sup>+</sup>

Intracellular levels of reduced and oxidized NAD<sup>+</sup> and NADP<sup>+</sup> were determined by the improved cyclic assay (Gibon and Larher, 1997) using either ADH (Sigma #A3263) or G6PDH (Sigma #G6378), respectively. Samples were prepared from 1 mL of culture rapidly collected as described by (Nikel et al., 2008; Chavarria et al., 2013), using cells cultivated either until the mid-log (OD<sub>600nm</sub> of 0.4–0.5) or late-log (OD<sub>600nm</sub> of 1.0–1.2) phases. Reduced and oxidized nicotinamide adenine dinucleotides were rapidly extracted by treatment with alkali or acid, respectively, followed by extract neutralization to avoid metabolic derived changes (London and Knight, 1966; Chavarria et al., 2013). The assay was performed in 200  $\mu$ L in a water bath for 30 min at 37°C. Reactions were stopped by addition of 100  $\mu$ L of 5 M NaCl followed by 5 min of ice incubation. The precipitated formazan was recovered by centrifugation for 5 min at 14,000  $\times$  g and solubilized in 500  $\mu$ L of 96% ethanol. Solubilized formazan was quantified as a function of the absorbance at 550 nm in a Biotek ELX-800 microplate reader. The standard calibration curve was set in triplicate following instructions given by Gibon and Larher (1997) using up to 30 pmol/assay of either NAD(P)H or NAD(P)<sup>+</sup>.

### Determination of Intracellular Adenine Nucleotides

Intracellular levels of adenine nucleotides were quantified using *H. seropedicae* strains grown as above until the mid-log phase (OD<sub>600nm</sub> of 0.4–0.5). Samples were prepared using cell pellets harvested from 1.5 mL by fast centrifugation at room temperature (15 s at 12,000  $\times$  g). The supernatant was discarded and the microcentrifuge tubes transferred to an ice-NaCl cooling bath at –20°C. Immediately, the metabolites were extracted resuspending the pellets in 200  $\mu$ L of 40:40:20 acetonitrile:methanol:water solvent system (at –20°C) with formic acid to a final concentration of 0.1 M as previously described (Bennett et al., 2008). The mixture was kept for 15 min at –20°C in an ice-NaCl cooling bath and then centrifuged for 5 min at 14,000  $\times$  g at 4°C for 5 min to pellet the insoluble material. The samples were analyzed by LC-MS. The chromatographic separation of metabolites was carried out injecting 10  $\mu$ L of the mix in a Kinetex C18 column (Phenomenex, United States) applying a gradient with the following solvents: (A) 97:3 water:methanol with 10 mM tributylamine and 15 mM acetic acid; (B) methanol using a

flow rate of 100  $\mu\text{L}/\text{min}$  (Lu et al., 2010). The  $m/z$  values of the ions were acquired in negative mode in a quadrupole-time of flight mass spectrometer (micrOTOF-Q II, Bruker Daltonics, United States). The parameters of the ESI source were set as following: capillary voltage 4,500 V, end plate offset voltage  $-500$  V, nebulizer pressure 2.0 bar, dry gas flow 6 L/min, drying gas temperature  $180^\circ\text{C}$ . The collision energy in the quadrupole was set 10 eV. The retention time for each adenine nucleotide was determined injecting standard solutions in different concentrations and monitoring the following ions: ATP,  $505.9957 \pm 0.05$   $m/z$ ; ADP  $426.0294 \pm 0.05$   $m/z$ ; and AMP  $346.0630 \pm 0.05$   $m/z$ .

## NMR Spectroscopy Determination of Malate and Acetate Levels in the Supernatant of Bacterial Cultures

Samples for NMR spectroscopy analysis were prepared as follows. A 200  $\mu\text{L}$  of  $\text{D}_2\text{O}$  were added to 400  $\mu\text{L}$  of supernatant media from bacterial cultures after centrifugation ( $12,000 \times g$  for 2 min).  $^1\text{H}$ -NMR spectra were acquired for each sample at 600 MHz (Ascend<sup>TM</sup> 600, Bruker) spectrometer equipped with a 5 mm QXI inverse probe and a Sample Case autosampler. The temperature was controlled at  $30^\circ\text{C}$  throughout the experiment. Standard  $^1\text{H}$ -NMR pulse sequence with water pre-saturation (Bruker pulse program zgpr) was applied to each sample. A total of 64 transient free induction decays (FID) were collected for each experiment with a spectral width of 20 ppm. The relaxation delay was set to 1 s. The  $90^\circ$  pulse length was automatically calibrated for each sample at around 11  $\mu\text{s}$ . The total acquisition time of each sample was 1 min 27 s. The metabolite concentrations were measured based on the height of the peaks in phosphate buffer pH 6.8: malate at  $\delta$  2.664 ( $\text{CH}_2$  doublet,  $\text{JH} \rightarrow \text{H} = 14.9$  Hz) and acetate at  $\delta$  1.904 ( $\text{CH}_3$  singlet).

## PHB Quantification

Quantification of PHB was performed by gas chromatography coupled to a flame-ionization detector essentially as described previously (Braunegg et al., 1978). In brief, acid methanolysis was performed with up to 10 mg of lyophilized bacterial cell pellets and then the derived 3-hydroxybutyric methyl ester (Me-3-HB) was dried with  $\text{Na}_2\text{SO}_4$ , and quantified by gas chromatography. The PHB amount in each sample was normalized by cell dry weight (cdw) and was expressed as % PHB/cdw. Alternatively, the PHB levels were quantified by Nile Red staining as described by (Zuriani et al., 2013). In brief, cells cultivated to late log phase were collected by centrifugation, resuspended in PBS (Sigma # P4417) and stained for 40 min at  $30^\circ\text{C}$  with 10  $\mu\text{g}/\text{mL}$  of Nile Red (Sigma # 72485) prepared in DMSO. After incubation, 200  $\mu\text{L}$  of cells were transferred to a 96-well black plate with clear bottom (Greiner Bio-One # 655096) and the fluorescence ( $\lambda_{\text{ex}}$ : 485 nm and  $\lambda_{\text{em}}$ : 535 nm) was measured on a Tecan Infinite 200 microplate reader.

## Heme Staining

Protein extracts from bacterial cultures grown under low aeration (120 rpm) were prepared exactly as described by Batista et al.

(2013). Fifty micrograms of protein were loaded without boiling onto a 15% Tris-Tricine SDS-PAGE gel, and stained using *o*-dianisidine for detection of covalently bound heme proteins (Francis and Becker, 1984).

## Analysis of Intracellular ROS Levels Using Flow Cytometry

*Herbaspirillum seropedicae* strains were grown as described above. Cells from 1 mL of culture were collected by centrifugation at  $14,000 \times g$  for 1 min and then resuspended in 500  $\mu\text{L}$  of PBS buffer supplemented with 1 mM EDTA, 0.01% Tween 20, and 0.1% Triton X-100. Cells were subsequently incubated with 50  $\mu\text{M}$  2',7'-dichlorodihydrofluorescein diacetate ( $\text{H}_2\text{-DCFDA}$ ) for 30 min at  $30^\circ\text{C}$  in the dark. Control experiments without  $\text{H}_2\text{-DCFDA}$  addition were also set up under the same conditions. Treatments with extra ROS source or with an antioxidant agent were also performed by pre-incubation of cells with 5 mM  $\text{H}_2\text{O}_2$  or with 5 mM *N*-acetyl-L-cysteine (Nac), respectively, for 30 min before addition of  $\text{H}_2\text{-DCFDA}$ . The samples were analyzed by flow cytometry using a BD Accuri<sup>TM</sup> C5 flow cytometer equipped with a 488 nm argon laser and a 533/30 nm bandpass filter (FL1-H). The median fluorescence intensity was used to determine the intracellular ROS levels.

## Analysis of Superoxide Levels by Fluorescence Microscopy

Aiming to access the levels of superoxide produced by *H. seropedicae* SmR1 and  $\Delta\text{phaC1}$  strains, fluorescence microscopy imaging was performed after treatment of the cells with superoxide specific probe dihydroethidium (DHE). Upon entry into the cells, DHE reacts with superoxide to form oxethidium (Zhao et al., 2003) which then interacts with nucleic acids emitting a bright red color detectable qualitatively by fluorescent microscope (Tarpey et al., 2004). Briefly, the bacterial cultures (1 mL) were harvested by centrifugation for 60 s at  $10,000 \times g$ , and the cell pellets were resuspended in 300  $\mu\text{L}$  of PBS buffer followed by addition of 3  $\mu\text{L}$  of 5 mM DHE dissolved in DMSO. After incubation for 30 min, the cells were visualized under a fluorescent microscope. The images were obtained using an Axio Imager Z2 microscope (Carl Zeiss Microscopy GmbH, Jena, Germany), equipped with four Metafer automated capture software (Metasystems GmbH, Altlußheim, Germany) and a CoolCube 1 camera (with  $100\times$  magnification). For fluorescence quantification, four images obtained from each strain (two for each biological replicate) were analyzed using the ImageJ software (Schneider et al., 2012) following the manufacturer's instructions. Briefly, after exporting the images into ImageJ software, the images were submitted to thresholding prior to particle (cell) analysis and fluorescence intensity counting. The fluorescence intensity for each particle was normalized by its area and then the sum of the normalized fluorescence intensity of all particles (cells) was finally divided by the total number of particles in each image. The software assigned between 200 and 300 particles in each analyzed image. The results are given as the mean  $\pm$  standard deviation from quantifications performed for four different images from each

strain. The normalized fluorescence intensity is given in arbitrary units (AU).

## RNA Isolation and RNA-Seq Library Construction

For total RNA extraction, *H. seropedicae* SmR1 (wild-type) and  $\Delta$ *phaC1* strains were grown to an optical density of approximately 1.0 (late-log phase), when high levels of PHB production occur (Tirapelle et al., 2013). Cells were collected by centrifugation and the total RNA was purified using the RNA RiboPure™-Bacteria kit (Ambion™) following the manufacturer's instructions. mRNA was enriched using the MICROExpress™ kit (Ambion™) performing two rounds of rRNA depletion. Up to 500 ng of mRNA enriched RNA was used for cDNA synthesis and library construction using the Ion Total RNA-Seq Kit v2 (Applied Biosystems™) following the manufacturer instructions. Sample multiplexing was performed using the Ion Xpress™RNA-Seq Barcode 1-16 Kit (Applied Biosystems™). The RNA-Seq libraries were sequenced on the Ion Proton™ (Applied Biosystems™).

## Read Mapping, Differential Expression Analysis, and Other Computational Analysis

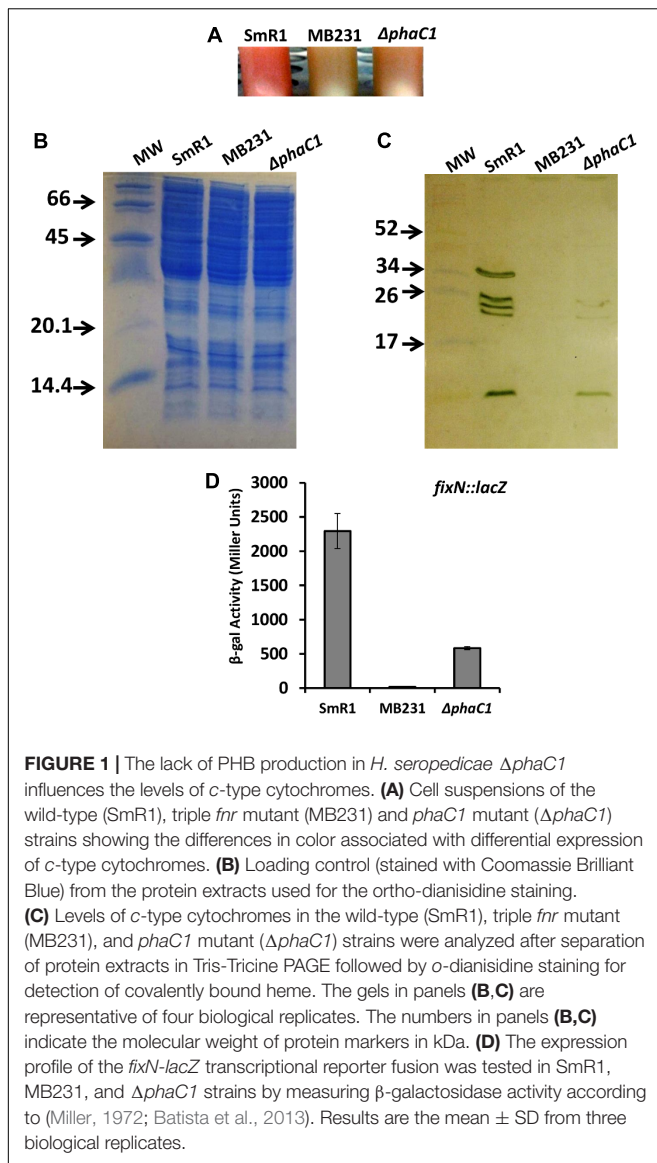
Reads were mapped against *H. seropedicae* SmR1 CDS (NC\_014323) using the CLC Genomics Workbench 7.0 (CLC bio). To increase the data robustness, two statistical methods for differential expression (DE) were used. The data set corresponding to the genes differentially expressed in both methods was used for further analysis. First, the DE analysis was performed using the RPKM normalization method (Mortazavi et al., 2008) and Baggerley beta-binomial statistics included in CLC Genomics Workbench 7.0. The output table was used for data filtering considering only genes with six times coverage in at least one of the strains. DE genes were those with a fold change of at least 2, and FDR lower than 0.05. For the second DE analysis, the read counts table was exported from CLC into the RobiNA software (Lohse et al., 2012) and statistical evaluation of differential gene expression was performed by DESeq (Anders and Huber, 2010) considering a *p*-value cut-off of 0.05 using the Benjamini–Hochberg method for multiple testing corrections. Similarly, to the first analysis, genes with fold changes lower than two were excluded. The final set of regulated genes is presented in Supplementary Table 2. To check which DE genes overlapped with the *H. seropedicae* Fnr regulon, we compared the current transcriptomic dataset with the published *H. seropedicae* *fnr* mutant dataset (Batista et al., 2013). Additionally, potential Fnr-binding sites in the *H. seropedicae* genome were inspected by using the *E. coli* Fnr protein binding motif (Myers et al., 2013) and the FIMO search tool with default parameters (Grant et al., 2011). Finally, the list of overlapping regulated genes between both datasets was compared to those genes containing promoters with potential Fnr-binding sites. Results showing the potential direct or indirect Fnr targets are presented in Supplementary Table 3. The sequence data for all libraries analyzed in this study are

available in ArrayExpress database under the accession number E-MTAB-5303.

## RESULTS

### Accumulation of PHB Is Physiologically Important for the Synthesis of *c*-Type Cytochromes

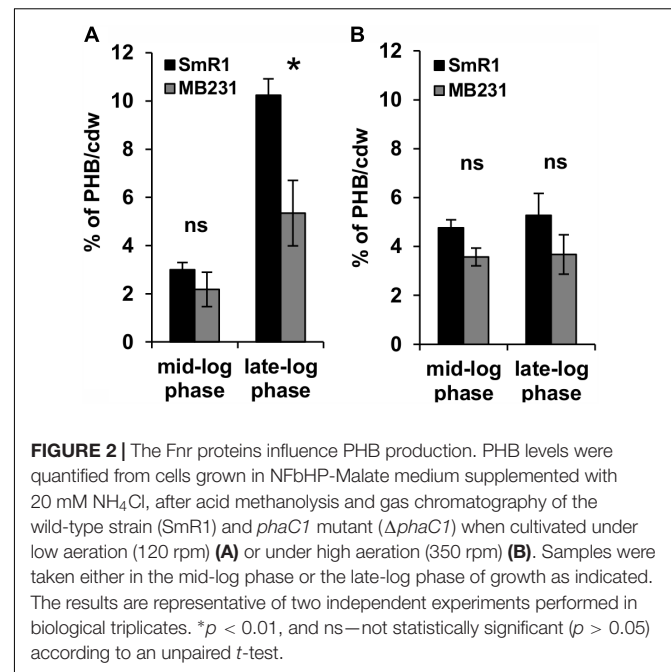
In *H. seropedicae* SmR1, the production of PHB is mainly dependent upon the PHA synthase encoded by *phaC1* (formerly *phbC1*; Tirapelle et al., 2013). Quantitative and qualitative analysis of PHB production by gas chromatography (Tirapelle et al., 2013) together with fluorescence and transmission microscopy (Alves et al., 2016) revealed that a strain with an in-frame deletion of *phaC1* is unable to produce PHB. This phenotype can be complemented *in trans* by the expression of *phaC1* from either a constitutive promoter or the native promoter (Supplementary Figure 1). Furthermore, whilst the *phaC1* gene is likely to form an operon with *phaB1* (Hsero\_2998), analysis of transcripts mapping to the *phaC1* (Hsero\_2999) neighborhood, suggests that in-frame deletion of *phaC1* does not affect the expression of immediate downstream genes, including *phaB1* (Hsero\_2998) and *phaR* (Hsero\_2997) (Supplementary Figure 2; see also Supplementary Table 2). Apart from being defective in PHB production, we observed that the *phaC1* deletion strain ( $\Delta$ *phaC1*) had a distinct phenotype conferred by lack of pink pigmentation when cultured in liquid media (Figure 1A). In *H. seropedicae* SmR1 this pigmentation is associated with *c*-type cytochromes, whose synthesis is dependent upon the redox-sensing proteins Fnr1 and Fnr3 (Batista et al., 2013). Therefore, we anticipated that the *phaC1* mutant strain would be defective in the expression of *c*-type cytochromes. To examine this hypothesis, we compared the heme-stained protein profile of the wild-type strain SmR1, with that of a triple *fnr* deletion strain (MB231) and the  $\Delta$ *phaC1* strain (Figures 1B,C). Similar to the triple *fnr* deletion, the *phaC1* deletion strain had reduced levels of all five cytochromes when compared to the wild-type strain (SmR1). The first and third bands (from the top to the bottom of the gel) were undetectable in the protein extracts of  $\Delta$ *phaC1*, while the other bands were significantly reduced (Figure 1C). As the synthesis of *c*-type cytochromes is mainly dependent upon the activity of the Fnr1 and Fnr3 regulatory proteins (Batista et al., 2013), it is possible that the absence of PHB imposes a physiological state that reduces transcriptional activation by Fnr proteins under oxygen-limiting conditions. To further validate the relationship between the absence of PHB and the activity of the Fnr proteins, we tested the expression of the *fixNOP* operon (encoding the *ccb*<sub>3</sub>-type oxidase) using a *fixN-lacZ* transcriptional fusion (Figure 1D; Batista et al., 2013). Comparing the expression profile of *fixNOP* in the strains SmR1, MB231, and  $\Delta$ *phaC1* (Figure 1D), transcriptional activation by Fnr1 and Fnr3 was clearly affected in the  $\Delta$ *phaC1* strain since the activity of the *fixN-lacZ* reporter was approximately 75% lower in this strain compared to the wild-type (Figure 1D). The reduction in *fixNOP* expression is in accordance with the



absence of band 1 (FixP; Batista et al., 2013) in the heme-stained gel (**Figure 1C**). Furthermore, the reduced expression of all five *c*-type cytochromes in the  $\Delta phaC1$  mutant also correlates with the growth penalty observed in this strain when the cells were cultured in 96-well microtiter plates, which limits oxygen diffusion and thus imposes oxygen-limiting conditions (Supplementary Figure 3).

### Deletion of the *fnr* Genes Affects PHB Production in *H. seropedicae* Under Oxygen-Limiting Conditions

Previous RNA-Seq based transcriptomic data revealed that the Fnr proteins are implicated in the expression of all three homologous PHA synthases in *H. seropedicae* (Batista et al., 2013). Transcripts mapping to the *phaC2* and *phaC3* genes were reduced by 100- and 60-fold respectively, while expression



of the *phaC1* gene was reduced by approximately threefold in the triple *fnr* mutant strain compared to the wild-type (Batista et al., 2013). In addition, the biosynthesis of PHB was earlier found to be influenced by CydR, an Fnr ortholog, in the diazotroph *Azotobacter vinelandii* (Wu et al., 2001). To address whether or not the *H. seropedicae* Fnr proteins are required for PHB production, we measured PHB levels in the triple *fnr* mutant under two different phases of growth and aeration regimes (**Figure 2**). When cells were grown under low aeration (120 rpm) and harvested in the mid-log phase, no difference in PHB production was observed between SmR1 and the triple *fnr* deletion strains. However, in late-log phase when the oxygen tension in the culture was reduced, the triple *fnr* deletion exhibited a significant reduction in PHB production (approximately 50%) compared to SmR1 (**Figure 2A**). In contrast, under high aeration (350 rpm), where oxygen levels are detrimental to Fnr activity (Supplementary Figure 4), no difference in the levels of PHB was observed (**Figure 2B**), regardless of the growth phase analyzed. These observations reinforce the importance of Fnr proteins for optimal production of PHB in *H. seropedicae*.

### Increased Oxidative Stress Is Observed in the Absence of PHB Accumulation

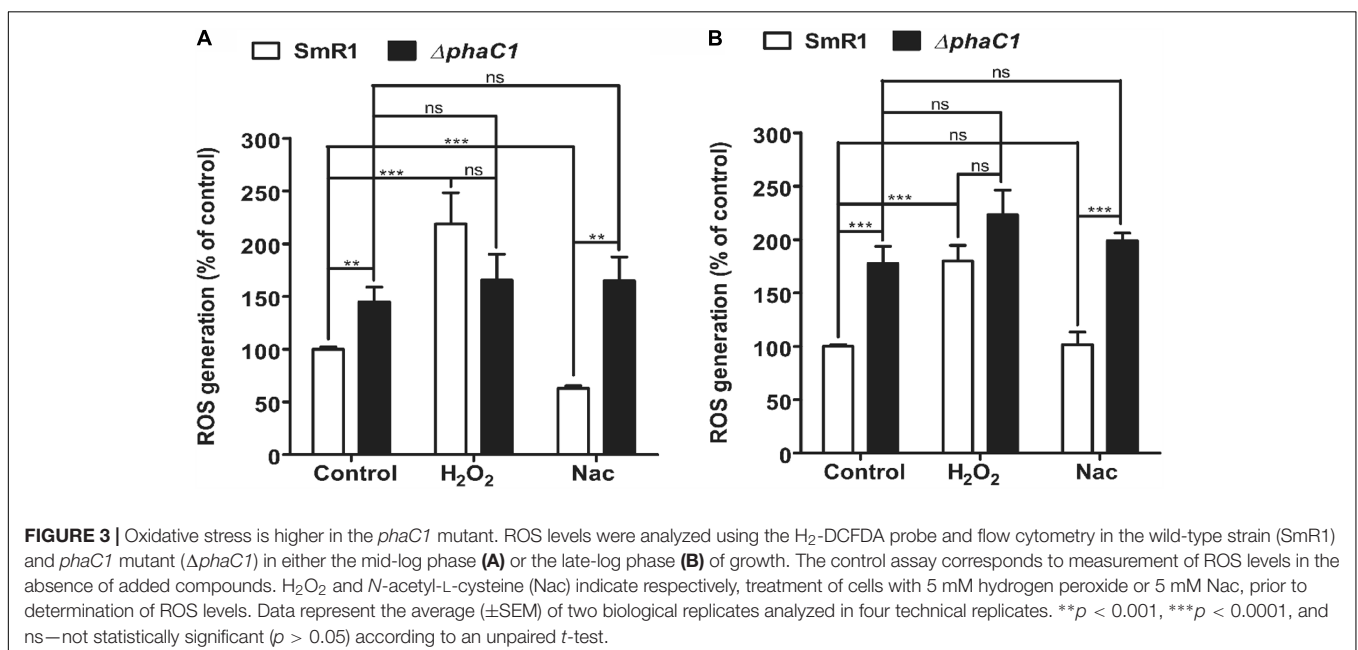
The decreased level of *c*-type cytochromes and the lower expression of the *fixN-lacZ* fusion (**Figure 1**) is apparently associated with a growth rate penalty in the *phaC1* mutant (Supplementary Figure 3), which implies that PHB accumulation is important for maintenance of Fnr activity in *H. seropedicae*. As the activity of Fnr is labile to oxygen and other ROS such as superoxide (Sutton et al., 2004; Crack et al., 2007), we were interested to know whether the *phaC1* mutant is subject to increased oxidative stress under low aeration. Using

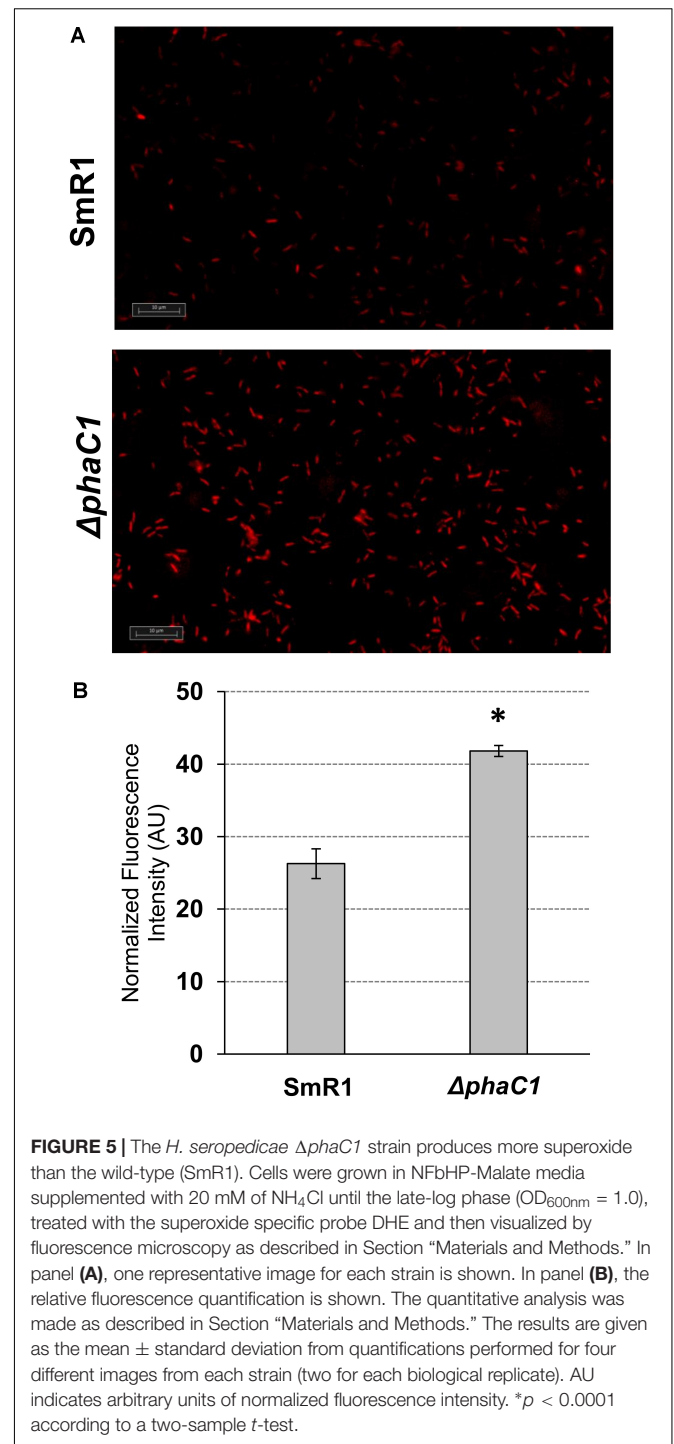
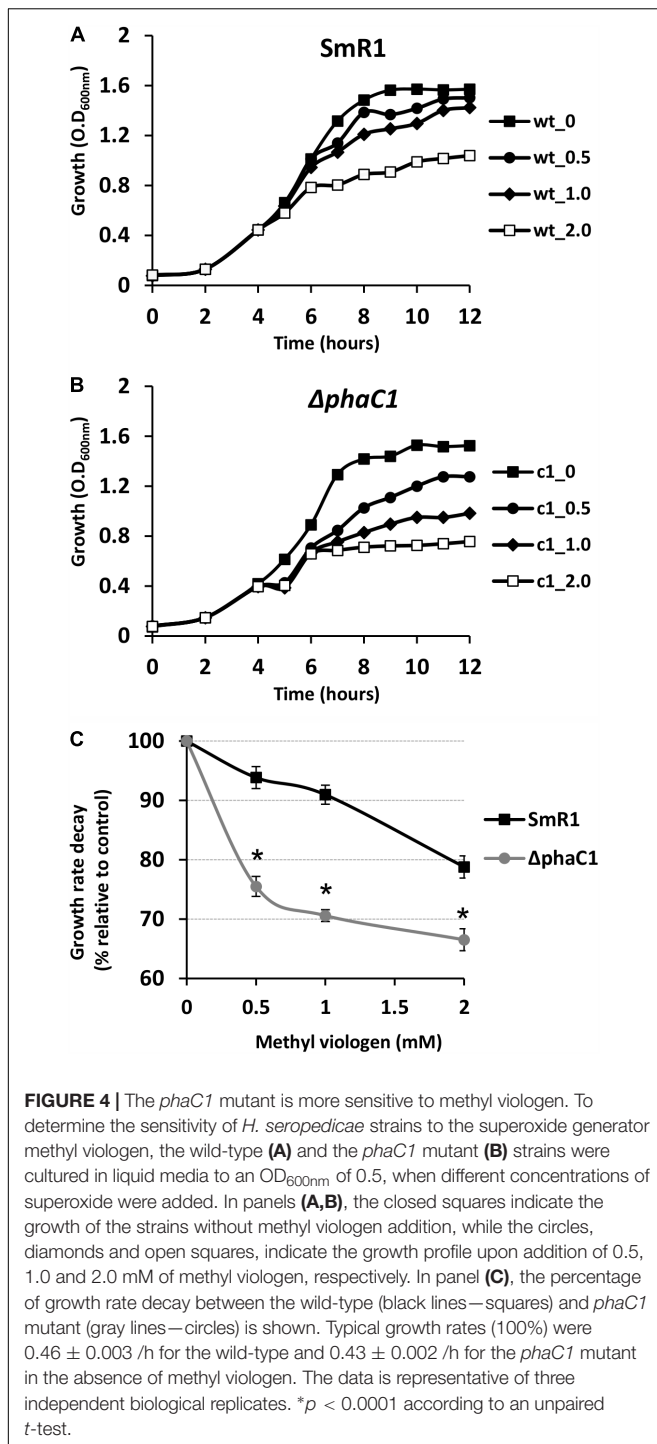
the fluorescent probe 2',7'-dichlorodihydrofluorescein diacetate (H<sub>2</sub>-DCFDA), we determined that the level of intracellular ROS was approximately 50% higher in the  $\Delta phaC1$  mutant, when cells were analyzed during the mid-log phase (OD<sub>600</sub> 0.4–0.5) and was 75% higher in the late-log phase (OD<sub>600</sub> 1.0–1.2) when compared with the wild-type strain (Figures 3A,B). After challenging the cells with 5 mM hydrogen peroxide, ROS levels increased in the wild-type strain, but did not change in the  $\Delta phaC1$  mutant regardless of the growth phase. We also tested the ability of both strains to mitigate the level of ROS after treatment with the chemical antioxidant Nac. This treatment enabled the SmR1 strain to reduce ROS by approximately 60% in the early-log phase (Figure 3A). However, in the late-log phase the antioxidant treatment did not result in relief of oxidative stress (Figure 3B). In contrast, for the  $\Delta phaC1$  strain, treatment with the antioxidant was unable to alleviate ROS in either growth phases (Figures 3A,B). Taken together, these observations suggest that in the absence of PHB, higher levels of ROS are induced in the  $\Delta phaC1$  mutant strain, which then influences the activity of the Fnr proteins. Moreover, the inability of the  $\Delta phaC1$  strain to relieve oxidative stress upon addition of a chemical antioxidant, suggests that ROS levels and the antioxidant defense mechanisms of the bacterium were saturated in both phases of growth. The increase in ROS levels in the  $\Delta phaC1$  mutant was observed only under oxygen limitation. When the cells were grown at 350 rpm (high O<sub>2</sub>), no difference in ROS was observed between the wild-type and  $\Delta phaC1$  strains. However, upon a shift from 350 to 120 rpm (high to low O<sub>2</sub>) the levels of ROS in the  $\Delta phaC1$  strain were higher than in the wild-type (Supplementary Figure 5) as observed in the assays shown in Figures 3A,B. In accordance with the observation that the  $\Delta phaC1$  deletion is subject to increased oxidative stress, we observed that *sodB* (Hsero\_1165), encoding superoxide dismutase, in addition

to *btuE* (Hsero\_3805) and *trxB1* (Hsero\_3504), encoding glutathione peroxidase and thioredoxin reductase respectively, were activated by approximately threefold in the  $\Delta phaC1$  mutant (Supplementary Figure 6 and Supplementary Table 2).

### Growth Inhibition by Superoxide Propagation Is More Severe in the $\Delta phaC1$ Strain

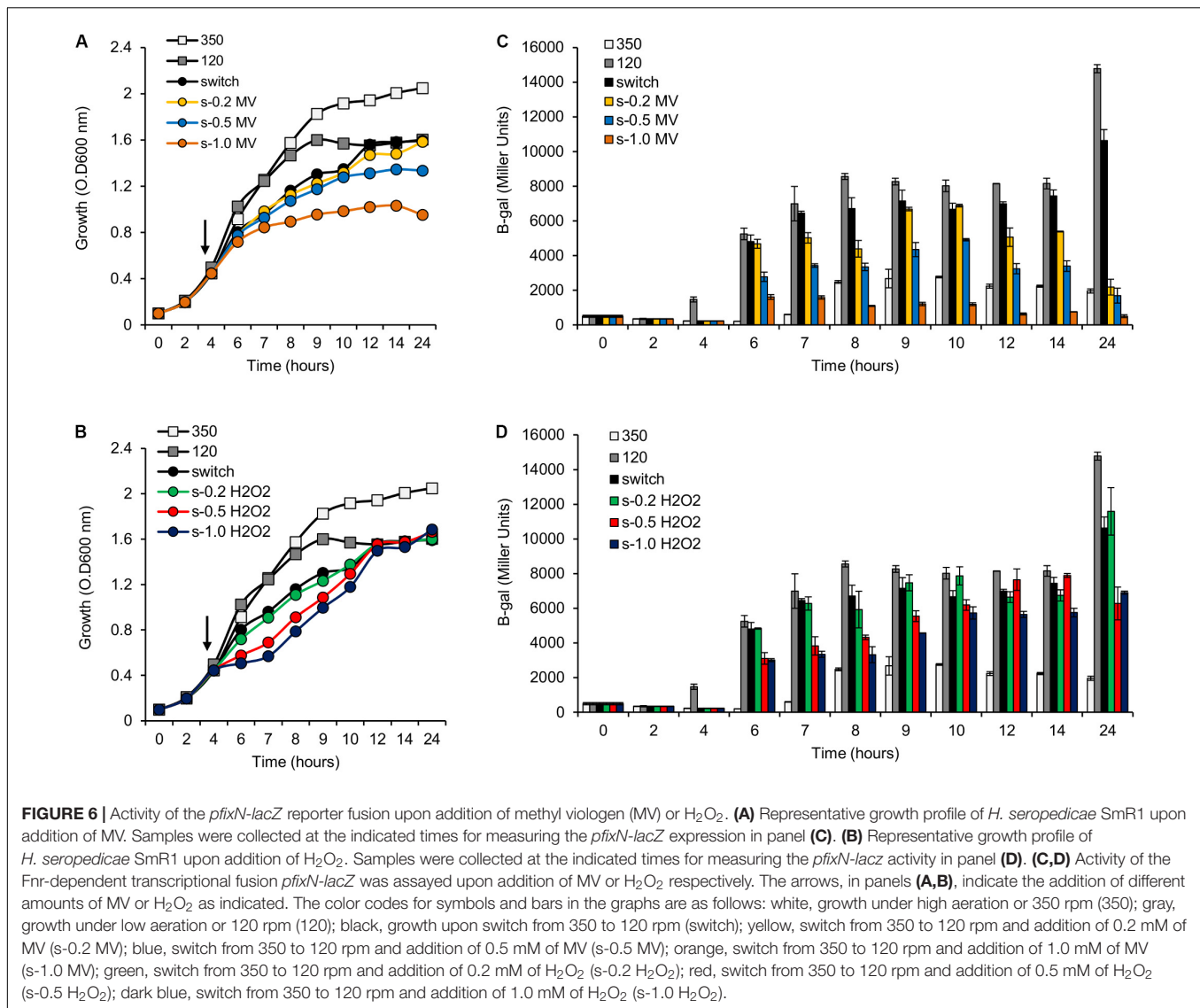
The results above demonstrate that mutation of the *phaC1* gene increases oxidative stress when cells are grown in laboratory conditions. However, in the natural environment, this bacterium would have to cope with external sources of ROS generated either by plants or by other competing organisms in the rhizosphere (Nanda et al., 2010; Sharma et al., 2012; Koskimäki et al., 2016). We therefore evaluated the growth phenotype of both wild-type and  $\Delta phaC1$  strains when an extra source of ROS was added to the culture media. When different concentrations of methyl viologen, a generator of intracellular superoxide (Gaudu and Fontecave, 1994), was added to the cultures, the  $\Delta phaC1$  mutant had a reduced growth rate compared to the wild-type (Figure 4). However, when a similar treatment was performed using H<sub>2</sub>O<sub>2</sub> as an alternative ROS source, no differences in growth rates between both strains were observed (Supplementary Figure 7). These observations imply that oxidative damage generated in the absence of PHB is perhaps related to increased levels of intracellular superoxide production. To gain further physiological support for this hypothesis, we compared the levels of superoxide production in the wild-type and  $\Delta phaC1$  strains by staining the cells with the superoxide specific probe DHE, followed by fluorescence microscopy visualization, as described in Section “Materials and Methods.” The fluorescence micrographs of the stained cells, clearly suggest that the levels of superoxide are higher in the  $\Delta phaC1$  strain (Figure 5).





In addition, cell suspensions of the  $\Delta phaC1$  strain showed brighter red fluorescence under UV-light when stained with DHE (Supplementary Figure 8), further supporting our hypothesis. Finally, considering that superoxide amplifies the oxidation of  $[4Fe-4S]^{2+}$  clusters (Sutton et al., 2004; Crack et al., 2007), we were interested to know whether additional levels of superoxide can affect the activity of the Fnr proteins in the wild-type strain. To examine this, we assayed the activity of the *fixN-lacZ*

transcriptional fusion, which is dependent upon both Fnr1 and Fnr3, following the addition of either methyl viologen or  $H_2O_2$  to the wild-type strain (Figure 6). While both oxidants were observed to reduce Fnr activity, the effect of methyl viologen was more pronounced, as the addition of 1.0 mM of methyl viologen was sufficient to reduce Fnr activity to similar levels to those observed in the  $\Delta phaC1$  mutant (Figures 1, 6). Altogether, these observations imply that increased levels of superoxide in the



$\Delta$ *phaC1* mutant correlate with inactivation of the Fnr proteins, as suggested by the results shown in **Figure 1**.

## The Redox Balance and the Energy Status Are Perturbed in the *phaC1* Deletion Strain

To investigate the relationship between PHB production and redox balance, we determined the levels of the pyridine nucleotide pool in the  $\Delta$ *phaC1* and wild-type strains during the mid-log and late-log phases of growth, corresponding to an OD<sub>600nm</sub> of 0.4–0.5 and 1.0–1.2, respectively, using cells cultured at 120 rpm (**Table 1**). During the mid-log phase, both NADPH/NADP<sup>+</sup> and NADH/NAD<sup>+</sup> ratios were increased by approximately two- and threefold, respectively, in the  $\Delta$ *phaC1* strain when compared to the wild-type. During the late-log phase, the NADH/NAD<sup>+</sup> ratio also increased in the  $\Delta$ *phaC1* strain (approximately threefold). In contrast, a slight decrease in the

NADPH/NADP<sup>+</sup> ratio was observed in the  $\Delta$ *phaC1* strain. The data presented in **Table 1** also reveal that the wild-type strain of *H. seropedicae* is able to undergo physiological adaptations to keep the NAD(P)H/NAD(P)<sup>+</sup> ratios almost constant during both the exponential and the late-log phase. In contrast, more significant fluctuations in the NAD(P)H/NAD(P)<sup>+</sup> ratios were observed in the *phaC1* mutant when pyridine nucleotide levels were compared in the two growth phases. The inability of the *phaC1* mutant to maintain the NAD(P)H/NAD(P)<sup>+</sup> ratios, exemplified by increased levels of reduced pyridine nucleotides (**Table 1**) may account for the exacerbated sensitivity of the mutant to oxidative stress (**Figures 3, 4**). In addition, we also investigated the levels of adenine nucleotides in both the *phaC1* mutant and wild-type strains by measuring the levels of AMP, ADP, and ATP as described in Section “Materials and Methods.” Interestingly ATP levels in the *phaC1* mutant were reduced by 2.3-fold when compared to the wild-type, while the levels of both ADP and AMP remained unaltered in both strains (**Figure 7**).

**TABLE 1** | Effect of the *phaC1* mutation on pyridine nucleotide pools at different growth phases.

Nucleotide pool	Mid-log phase		Late-log phase	
	Wild-type	$\Delta phaC1$	WT	$\Delta phaC1$
NADH	1.68 ± 0.28 <sup>a</sup>	2.31 ± 0.26	0.64 ± 0.10	1.74 ± 0.16
NAD <sup>+</sup>	29.38 ± 3.57	21.07 ± 2.95	13.48 ± 1.10	11.31 ± 2.26
NADH/NAD <sup>+</sup>	0.06	0.11	0.05	0.15
NADPH	2.22 ± 0.28	3.63 ± 0.68	1.32 ± 0.22	1.53 ± 0.15
NADP <sup>+</sup>	5.58 ± 0.55	2.90 ± 0.41	2.69 ± 0.46	3.83 ± 0.31
NADPH/NADP <sup>+</sup>	0.40	1.25	0.49	0.40

<sup>a</sup> pmol/μg/protein ± SD of four assays performed in biological replicates.

## Transcriptional Profiling Indicates That Deletion of *phaC1* Influences Expression of the Fnr Regulon

To examine the effect of the *phaC1* mutation on gene expression, we carried out RNA-Seq based transcriptome analysis using late log-phase cultures of the  $\Delta phaC1$  and wild-type strains, when the peak of PHB production is observed under our experimental conditions (Tirapelle et al., 2013). Analysis of transcripts mapping to *H. seropedicae* revealed that 678 genes were differentially expressed (Supplementary Table 2). From these, 276 were downregulated, while 402 were upregulated in the *phaC1* mutant strain. Approximately 60 of the differentially expressed genes are direct or indirect targets for Fnr1 and Fnr3 proteins (Supplementary Table 3) previously identified in the transcriptome analysis of the triple *fnr* mutant strain (Batista et al., 2013). Some of these genes are likely to be directly regulated by Fnr, since Fnr binding motifs were found upstream of the promoters using a FIMO motif search (Grant et al., 2011). The Fnr regulon in *H. seropedicae* comprises 187 genes (Batista et al., 2013), with the *phaC1* mutation influencing about 30% of these genes.

## Metabolic Changes Triggered in the *phaC1* Mutant

During the colonization of a given environment, limitations in oxygen availability may be encountered as a consequence of cell density increases and the metabolic activity of competing organisms. Under such conditions decreased electron flux through the ETC may occur, with concomitant reduction in the consumption of reducing equivalents. To avoid the stress generated by imbalanced levels of reducing equivalents, the wild-type strain diverts acetyl-CoA from the TCA cycle and NAD(P)H from the ETC into the biosynthesis of PHB. As the *phaC1* mutant is unable to operate this mechanism, we tried to address how excessive accumulation of acetyl-CoA and NAD(P)H is avoided in the absence of PHB production, by quantifying metabolites in culture supernatants. Surprisingly, we found that the consumption of malate from the culture media does not differ between the wild-type and  $\Delta phaC1$  strains during various stages of growth (Figure 8). However, we observed that acetate levels in culture supernatants were approximately twofold higher

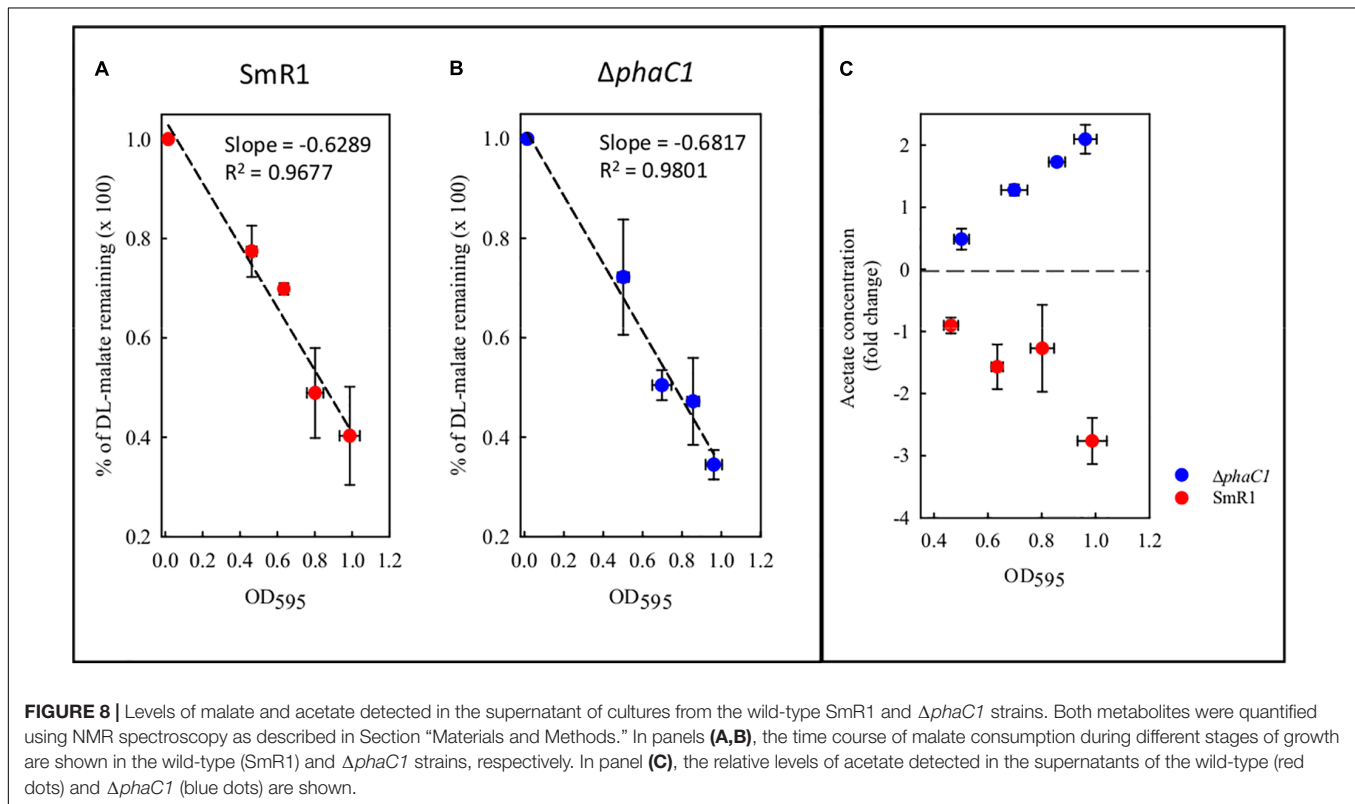
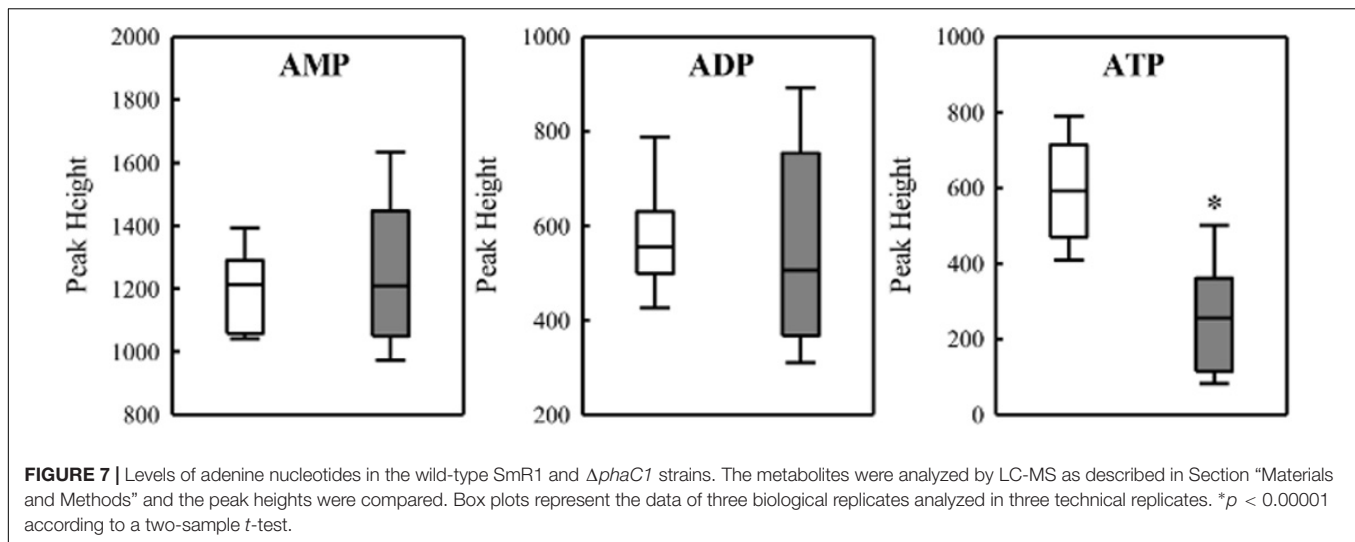
in the *phaC1* mutant strain when compared to the wild-type (Figure 8).

## DISCUSSION

In this study, we have determined the physiological importance of PHB for maintenance of the redox equilibrium in *H. seropedicae*. Transcription profiling of the  $\Delta phaC1$  mutant together with further physiological characterization suggests that in the absence of PHB synthesis, oxidative stress is exacerbated by increased levels of superoxide. This, in turn, correlates with partial inactivation of the Fnr proteins. The imbalance in the NAD(P)H/NAD(P)<sup>+</sup> ratios observed in the *phaC1* mutant is likely to be responsible for increased generation of superoxide, either by Complex I (Hirst et al., 2008; Pryde and Hirst, 2011) or Complex III (Lanciano et al., 2013). In *Rhodobacter sphaeroides*, the rate of superoxide generation by Complex III is modulated by the universal stress protein UspA (Su et al., 2015). Interestingly, a gene encoding a homolog of *R. sphaeroides* UspA (Hsero\_2299) was downregulated 10-fold in the *phaC1* mutant (Supplementary Table 2). Additionally, the decreased level of ATP in the *phaC1* mutant concurs with our observation that this mutant has reduced levels of *c*-type cytochromes (Figure 1), which are important for fine-tuning the electron flux in the respiratory chain, in order to maintain normal levels of ATP synthesis and facilitate growth under oxygen-limiting conditions.

Our results show that in *H. seropedicae*, and most likely in other PHA-producing bacteria, biosynthesis of PHB is used to divert acetyl-CoA and NAD(P)H from the TCA cycle and the ETC, respectively, thus serving as an alternative electron sink to allow the elimination of excess acetyl-CoA and reducing equivalents. How exactly the partitioning mechanism between TCA cycle and PHB biosynthesis operates has yet to be elucidated, but it is likely that a combination of factors controlling acetyl-CoA/CoA and NAD(P)H/NAD(P)<sup>+</sup> ratios, in addition to maintenance of the TCA cycle are major players in this mechanism (Trainer and Charles, 2006). In *H. seropedicae* SmR1, the aconitase enzyme was found to interact with PHB granules (Tirapelle et al., 2013). Perhaps, sequestration of aconitase during PHB production might control TCA cycle activity, thus helping to operate the partitioning mechanism. The *phaC1* mutant is apparently unable to operate this partitioning mechanism, resulting in increased levels of acetate excretion. Although acetate overflow may help to drain carbon, it does not apparently relieve the redox imbalance that generates oxidative stress.

Expression of protein complexes important for both the synthesis and activity of the cytochrome *c* branch of the ETC is dependent upon the Fnr1 and Fnr3 proteins in *H. seropedicae* SmR1 (Batista et al., 2013). Additionally, Fnr proteins are required for transcriptional activation of all three genes encoding PHA synthases in this organism (Batista et al., 2013). Therefore, it is feasible that regulation of the redox balance is primarily controlled by the Fnr proteins, since optimal PHB production and respiration at low oxygen concentrations are dependent upon Fnr. Conversely, the activation of PHB synthesis as an electron



sink is necessary to prevent oxidative stress and consequent impairment of Fnr-dependent transcriptional regulation. Thus, PHB synthesis and maintenance of Fnr activity exhibit cyclic dependency in *H. seropedicae*, since transcriptional activation by Fnr proteins is essential for full levels of PHB synthesis, whilst production of PHB is essential to prevent inactivation of Fnr. Recently, another link between PHB synthesis and transcriptional regulation by Fnr-like proteins was suggested in *Sinorhizobium meliloti* Rm1021. It was found that different mutants deficient in PHB synthesis and accumulation exhibited reduced transcript

levels of various genes associated with the presence of an Fnr-like regulatory sequence in their respective promoters (D'Alessio et al., 2017). It is therefore conceivable that a similar cyclic dependency between PHB synthesis and activity of Fnr-like proteins occurs in *S. meliloti* Rm102, to link the control of the PHB cycle with the activity of redox-sensitive regulatory circuits.

The influence of PHB synthesis on the Fnr regulon under conditions of oxygen limitation could perhaps provide a mechanism for shutting down expression of superoxide-generating components of the ETC when there is insufficient

carbon available to divert electrons into PHB synthesis. The use of an electron sink appears to be an important mechanism for *H. seropedicae* to adapt to changes in the redox status imposed by the environment. For example, in the presence of nitrate as nitrogen source, the respiratory nitrate reductase (NAR—encoded by *narGHJI* operon), is activated by the Fnr1 and Fnr3 proteins (Batista et al., 2013; Bonato et al., 2016). The reduction of nitrate by NAR also appears to be used as an electron sink in addition to PHB synthesis, since *H. seropedicae* is unable to respire nitrate under anaerobiosis (Bonato et al., 2016).

The findings reported here regarding the physiological significance of PHB together with the observation that the *phaC1* mutant has decreased competitiveness during plant colonization (Balsanelli et al., 2015) indicates that PHB plays an important role in cellular metabolism, not only under free-living conditions but also during the *Herbaspirillum*-plant interaction. PHB may be required to support redox homeostasis, thus allowing efficient bacterial competition in the rhizosphere and increased fitness for the early stages of the interaction with crops. In *H. seropedicae* and possibly other PHA-producing bacteria, the link between redox equilibrium and PHB synthesis is tightly controlled. Interestingly, it was recently found that increased levels of NADPH in an *ntnC* mutant of *H. seropedicae* led to higher PHB production and increased fitness toward oxidative stress (Sacomboio et al., 2017). Finally, the transcriptional changes uncovered here, together with increased knowledge of PHB metabolism in *H. seropedicae*, may enable engineering of more efficient PHB-producing strains, with potential biotechnological applications, including production of biodegradable plastics and development of bacterial inoculants with improved competitiveness in the rhizosphere.

## AUTHOR CONTRIBUTIONS

MB, CT, and MM-S designed and performed experiments, analyzed the data, and wrote the manuscript. MZS prepared

## REFERENCES

- Alves, L. P., Teixeira, C. S., Tirapelle, E. F., Donatti, L., Tadra-Sfeir, M. Z., Steffens, M. B., et al. (2016). Backup expression of the *PhaP2* phasin compensates for *phaP1* deletion in *Herbaspirillum seropedicae*, maintaining fitness and PHB accumulation. *Front. Microbiol.* 7:739. doi: 10.3389/fmicb.2016.00739
- Anders, S., and Huber, W. (2010). Differential expression analysis for sequence count data. *Genome Biol.* 11:R106. doi: 10.1186/gb-2010-11-10-r106
- Balsanelli, E., Tadra-Sfeir, M. Z., Faoro, H., Pankievicz, V. C. S., de Baura, V. A., Pedrosa, F. O., et al. (2015). Molecular adaptations of *Herbaspirillum seropedicae* during colonization of the maize rhizosphere. *Environ. Microbiol.* 18, 2343–2356. doi: 10.1111/1462-2920.12887
- Batista, M. B., Müller-Santos, M., Pedrosa, F. D. O., and de Souza, E. M. (2016). “Potentiality of *Herbaspirillum seropedicae* as a platform for bioplastic production,” in *Microbial Models: from Environmental to Industrial Sustainability*, ed. S. Castro-Sowinski (Singapore: Springer), 23–39. doi: 10.1007/978-981-10-2555-6\_2
- Batista, M. B., Sfeir, M. Z., Faoro, H., Wassem, R., Steffens, M. B., Pedrosa, F. O., et al. (2013). The *Herbaspirillum seropedicae* SmR1 Fnr orthologs controls the cytochrome composition of the electron transport chain. *Sci. Rep.* 3:2544. doi: 10.1038/srep02544
- Bennett, B. D., Yuan, J., Kimball, E. H., and Rabinowitz, J. D. (2008). Absolute quantitation of intracellular metabolite concentrations by an isotope ratio-based approach. *Nat. Protoc.* 3, 1299–1311. doi: 10.1038/nprot.2008.107
- Bonato, P., Batista, M. B., Camilios-Neto, D., Pankievicz, V. C. S., Tadra-Sfeir, M. Z., Monteiro, R. A., et al. (2016). RNA-seq analyses reveal insights into the function of respiratory nitrate reductase of the diazotroph *Herbaspirillum seropedicae*. *Environ. Microbiol.* 18, 2677–2688. doi: 10.1111/1462-2920.13422
- Braunegg, G., Sonnleimer, B., and Lafferty, R. (1978). A rapid gas chromatographic method for the determination of poly- $\beta$ -hydroxybutyric acid in microbial biomass. *Eur. J. Appl. Microbiol. Biotechnol.* 6, 29–37. doi: 10.1007/bf00500854
- Chavarría, M., Nikel, P. I., Perez-Pantoja, D., and de Lorenzo, V. (2013). The Entner-Doudoroff pathway empowers *Pseudomonas putida* KT2440 with a high tolerance to oxidative stress. *Environ. Microbiol.* 15, 1772–1785. doi: 10.1111/1462-2920.12069
- Chubatsu, L. S., Monteiro, R. A., Souza, E. M., Oliveira, M. A. S., Yates, M. G., Wassem, R., et al. (2011). Nitrogen fixation control in *Herbaspirillum seropedicae*. *Plant Soil* 356, 197–207. doi: 10.1007/s11104-011-0819-6
- Crack, J. C., Green, J., Cheesman, M. R., Le Brun, N. E., and Thomson, A. J. (2007). Superoxide-mediated amplification of the oxygen-induced switch from [4Fe-4S] to [2Fe-2S] clusters in the transcriptional regulator FNR. *Proc. Natl. Acad. Sci. U.S.A.* 104, 2092–2097. doi: 10.1073/pnas.0609514104
- D’Alessio, M., Nordeste, R., Doxey, A. C., and Charles, T. C. (2017). Transcriptome analysis of polyhydroxybutyrate cycle mutants reveals discrete loci connecting

and sequenced RNA-Seq libraries. LA performed PHB quantifications and the fluorescence microscopy. GV performed ROS quantification experiments. GS performed metabolite quantification by NMR spectroscopy. FOP, MBS, and ES conceived the idea of the project and analyzed the data. RD and MM-S supervised the study, analyzed the data, and wrote the manuscript.

## FUNDING

This research was funded by CNPq (Brazilian National Council for Scientific and Technological Development), project “Investigação do Papel das Proteínas Fasin na Biossíntese de Polihidroxialcanoatos e na Resposta Anti-Estresse em Bactérias” process 458417/2014-9. This study was supported by the Brazilian Program of National Institute of Science and Technology for Biological Nitrogen Fixation (INCT-FBN)/Brazilian Research Council-CNPq/MCT, Fundação Arauária and CAPES. RD and MB were supported by the UK Biotechnology and Biosciences Research Council (BBSRC) grant number BB/N013476/1.

## ACKNOWLEDGMENTS

Roseli A. Prado, Marilza D. Lamour, and Valter A. de Baura are acknowledged for technical assistance to the Nitrogen Fixation Group. We are also in debt to Lisandra Maba and Israel Bini from the Cell Biology Department of the UFPR, for assistance with the fluorescence microscope.

## SUPPLEMENTARY MATERIAL

The Supplementary Material for this article can be found online at: <https://www.frontiersin.org/articles/10.3389/fmicb.2018.00472/full#supplementary-material>

- nitrogen utilization and carbon storage in *Sinorhizobium meliloti*. *mSystems* 2:e00035-17. doi: 10.1128/mSystems.00035-17
- Francis, R. T. Jr., and Becker, R. R. (1984). Specific indication of hemoproteins in polyacrylamide gels using a double-staining process. *Anal. Biochem.* 136, 509–514. doi: 10.1016/0003-2697(84)90253-7
- Gaudu, P., and Fontecave, M. (1994). The NADPH: sulfite reductase of *Escherichia coli* is a paraquat reductase. *Eur. J. Biochem.* 226, 459–463. doi: 10.1111/j.1432-1033.1994.tb20070.x
- Gibon, Y., and Larher, F. (1997). Cycling assay for nicotinamide adenine dinucleotides: NaCl precipitation and ethanol solubilization of the reduced tetrazolium. *Anal. Biochem.* 251, 153–157. doi: 10.1006/abio.1997.2283
- Grant, C. E., Bailey, T. L., and Noble, W. S. (2011). FIMO: scanning for occurrences of a given motif. *Bioinformatics* 27, 1017–1018. doi: 10.1093/bioinformatics/btr064
- Hirst, J., King, M. S., and Pryde, K. R. (2008). The production of reactive oxygen species by complex I. *Biochem. Soc. Trans.* 36, 976–980. doi: 10.1042/bst0360976
- Kadouri, D., Jurkevitch, E., and Okon, Y. (2003). Involvement of the reserve material poly-beta-hydroxybutyrate in *Azospirillum brasilense* stress endurance and root colonization. *Appl. Environ. Microbiol.* 69, 3244–3250. doi: 10.1128/AEM.69.6.3244-3250.2003
- Klassen, G., Pedrosa, F. O., Souza, E. M., Funayama, S., and Rigo, L. U. (1997). Effect of nitrogen compounds on nitrogenase activity in *Herbaspirillum seropedicae* SmR1. *Can. J. Microbiol.* 43, 887–891. doi: 10.1139/m97-129
- Koskimäki, J. J., Kajula, M., Hokkanen, J., Ihanntola, E. L., Kim, J. H., Hautajarvi, H., et al. (2016). Methyl-esterified 3-hydroxybutyrate oligomers protect bacteria from hydroxyl radicals. *Nat. Chem. Biol.* 12, 332–338. doi: 10.1038/nchembio.2043
- Lanciano, P., Khalfaoui-Hassani, B., Selamoglu, N., Ghelli, A., Rugolo, M., and Daldal, F. (2013). Molecular mechanisms of superoxide production by complex III: a bacterial versus human mitochondrial comparative case study. *Biochim. Biophys. Acta* 1827, 1332–1339. doi: 10.1016/j.bbabi.2013.03.009
- Lohse, M., Bolger, A. M., Nagel, A., Fernie, A. R., Lunn, J. E., Stitt, M., et al. (2012). RobiNA: a user-friendly, integrated software solution for RNA-Seq-based transcriptomics. *Nucleic Acids Res.* 40, W622–W627. doi: 10.1093/nar/gks450
- London, J., and Knight, M. (1966). Concentrations of nicotinamide nucleotide coenzymes in micro-organisms. *J. Gen. Microbiol.* 44, 241–254. doi: 10.1099/00221287-44-2-241
- Lopez, N. I., Pettinari, M. J., Nikel, P. I., and Mendez, B. S. (2015). Polyhydroxyalkanoates: much more than biodegradable plastics. *Adv. Appl. Microbiol.* 93, 73–106. doi: 10.1016/bs.aams.2015.06.001
- Lu, W., Clasquin, M. F., Melamud, E., Amador-Noguez, D., Caudy, A. A., and Rabinowitz, J. D. (2010). Metabolomic analysis via reversed-phase ion-pairing liquid chromatography coupled to a stand alone orbitrap mass spectrometer. *Anal. Chem.* 82, 3212–3221. doi: 10.1021/ac902837x
- Madison, L. L., and Huisman, G. W. (1999). Metabolic engineering of poly(3-hydroxyalkanoates): from DNA to plastic. *Microbiol. Mol. Biol. Rev.* 63, 21–53.
- Miller, J. H. (1972). *Experiments in Molecular Genetics*, 1st Edn. Cold Spring Harbor, NY: Cold Spring Harbor Laboratory Press.
- Mortazavi, A., Williams, B. A., McCue, K., Schaeffer, L., and Wold, B. (2008). Mapping and quantifying mammalian transcriptomes by RNA-Seq. *Nat. Methods* 5, 621–628. doi: 10.1038/nmeth.1226
- Myers, K. S., Yan, H., Ong, I. M., Chung, D., Liang, K., Tran, F., et al. (2013). Genome-scale analysis of *Escherichia coli* FNR reveals complex features of transcription factor binding. *PLoS Genet.* 9:e1003565. doi: 10.1371/journal.pgen.1003565
- Nanda, A. K., Andrio, E., Marino, D., Pauly, N., and Dunand, C. (2010). Reactive oxygen species during plant-microorganism early interactions. *J. Integr. Plant Biol.* 52, 195–204. doi: 10.1111/j.1744-7909.2010.00933.x
- Nikel, P. I., Pettinari, M. J., Ramirez, M. C., Galvagno, M. A., and Mendez, B. S. (2008). *Escherichia coli* arcA mutants: metabolic profile characterization of microaerobic cultures using glycerol as a carbon source. *J. Mol. Microbiol. Biotechnol.* 15, 48–54. doi: 10.1159/000111992
- Pedrosa, F. O., Monteiro, R. A., Wassem, R., Cruz, L. M., Ayub, R. A., Colauto, N. B., et al. (2011). Genome of *Herbaspirillum seropedicae* strain SmR1, a specialized diazotrophic endophyte of tropical grasses. *PLoS Genet.* 7:e1002064. doi: 10.1371/journal.pgen.1002064
- Pryde, K. R., and Hirst, J. (2011). Superoxide is produced by the reduced flavin in mitochondrial complex I: a single, unified mechanism that applies during both forward and reverse electron transfer. *J. Biol. Chem.* 286, 18056–18065. doi: 10.1074/jbc.M110.186841
- Quelas, J. I., Mongiardini, E. J., Perez-Gimenez, J., Parisi, G., and Lodeiro, A. R. (2013). Analysis of two polyhydroxyalkanoate synthases in *Bradyrhizobium japonicum* USDA 110. *J. Bacteriol.* 195, 3145–3155. doi: 10.1128/JB.02203-12
- Rehm, B. H. (2003). Polyester synthases: natural catalysts for plastics. *Biochem. J.* 376, 15–33. doi: 10.1042/BJ20031254
- Sacomboio, E. N. M., Kim, E. Y. S., Correa, H. L. R., Bonato, P., Pedrosa, F. O., de Souza, E. M., et al. (2017). The transcriptional regulator NtrC controls glucose-6-phosphate dehydrogenase expression and polyhydroxybutyrate synthesis through NADPH availability in *Herbaspirillum seropedicae*. *Sci. Rep.* 7:13546. doi: 10.1038/s41598-017-12649-0
- Schneider, C. A., Rasband, W. S., and Eliceiri, K. W. (2012). NIH Image to ImageJ: 25 years of image analysis. *Nat. Methods* 9, 671–675. doi: 10.1038/nmeth.2089
- Senior, P. J., Beech, G. A., Ritchie, G. A., and Dawes, E. A. (1972). The role of oxygen limitation in the formation of poly-β-hydroxybutyrate during batch and continuous culture of *Azotobacter beijerinckii*. *Biochem. J.* 128, 1193–1201. doi: 10.1042/bj1281193
- Sharma, P., Jha, A. B., Dubey, R. S., and Pesarakli, M. (2012). Reactive oxygen species, oxidative damage, and antioxidative defense mechanism in plants under stressful conditions. *J. Bot.* 2012:217037. doi: 10.1155/2012/217037
- Stockdale, H., Ribbons, D. W., and Dawes, E. A. (1968). Occurrence of poly-beta-hydroxybutyrate in the *Azotobacteriaceae*. *J. Bacteriol.* 95, 1798–1803.
- Su, T., Wang, Q., Yu, L., and Yu, C. A. (2015). Universal stress protein regulates electron transfer and superoxide generation activities of the cytochrome bc1 complex from *Rhodobacter sphaeroides*. *Biochemistry* 54, 7313–7319. doi: 10.1021/acs.biochem.5b00658
- Sutton, V. R., Stubna, A., Patschkowski, T., Munck, E., Beinert, H., and Kiley, P. J. (2004). Superoxide destroys the [2Fe-2S]<sup>2+</sup> cluster of FNR from *Escherichia coli*. *Biochemistry* 43, 791–798. doi: 10.1021/bi0357053
- Tarpey, M. M., Wink, D. A., and Grisham, M. B. (2004). Methods for detection of reactive metabolites of oxygen and nitrogen: in vitro and in vivo considerations. *Am. J. Physiol. Regul. Integr. Comp. Physiol.* 286, R431–R444. doi: 10.1152/ajpregu.00361.2003
- Tirapelle, E. F., Muller-Santos, M., Tadra-Sfeir, M. Z., Kadowaki, M. A., Steffens, M. B., Monteiro, R. A., et al. (2013). Identification of proteins associated with polyhydroxybutyrate granules from *Herbaspirillum seropedicae* SmR1 - old partners, new players. *PLoS One* 8:e75066. doi: 10.1371/journal.pone.0075066
- Trainer, M. A., and Charles, T. C. (2006). The role of PHB metabolism in the symbiosis of rhizobia with legumes. *Appl. Microbiol. Biotechnol.* 71, 377–386. doi: 10.1007/s00253-006-0354-1
- Wu, G., Moir, A. J., Sawers, G., Hill, S., and Poole, R. K. (2001). Biosynthesis of poly-beta-hydroxybutyrate (PHB) is controlled by CydR (Fnr) in the obligate aerobic *Azotobacter vinelandii*. *FEMS Microbiol. Lett.* 194, 215–220.
- Zhao, H., Kalivendi, S., Zhang, H., Joseph, J., Nithipatikom, K., Vasquez-Vivar, J., et al. (2003). Superoxide reacts with hydroethidine but forms a fluorescent product that is distinctly different from ethidium: potential implications in intracellular fluorescence detection of superoxide. *Free Radic. Biol. Med.* 34, 1359–1368. doi: 10.1016/S0891-5849(03)00142-4
- Zuriani, R., Vigneswari, S., Azizan, M. N. M., Majid, M. I. A., and Amirul, A. A. (2013). A high throughput Nile red fluorescence method for rapid quantification of intracellular bacterial polyhydroxyalkanoates. *Biotechnol. Bioeng. Proc.* 18, 472–478. doi: 10.1007/s12257-012-0607-z

**Conflict of Interest Statement:** The authors declare that the research was conducted in the absence of any commercial or financial relationships that could be construed as a potential conflict of interest.

Copyright © 2018 Batista, Teixeira, Sfeir, Alves, Valdameri, Pedrosa, Sasaki, Steffens, de Souza, Dixon and Müller-Santos. This is an open-access article distributed under the terms of the Creative Commons Attribution License (CC BY). The use, distribution or reproduction in other forums is permitted, provided the original author(s) and the copyright owner are credited and that the original publication in this journal is cited, in accordance with accepted academic practice. No use, distribution or reproduction is permitted which does not comply with these terms.